ECS Transactions, 7 (1) 2239-2244 (2007)
10.1149/1.2729340, ©The Electrochemical Society

Microstructure and Electrical Conductivity of $Ce_{0.85}Y_{0.15-x}RE_xO_{2-\delta}$ (RE = Pr, Tb)

S. K. Tadokoro and E. N. S. Muccillo

Centro de Ciência e Tecnologia de Materiais
Instituto de Pesquisas Energéticas e Nucleares, S. Paulo, SP, 05508000, Brazil

Solid solutions of $Ce_{0.85}Y_{0.15-x}RE_xO_{2-\delta}$ (RE=Pr,Tb) with x = 0.02 and 0.06 were synthesized by coprecipitation technique to study the effect of Pr and Tb additions on the microstructure and electrical conductivity of yttria-doped ceria (YDC) electrolyte. For comparison purposes, the solid solution $Ce_{0.85}Y_{0.13}Pr_{0.02}O_{2-\delta}$ was prepared by mixing Pr_6O_{11} to the precipitated gel of ceria-yttria. Reductions in the average grain size and in the full width at half maximum height of the grain size distribution curve were obtained with increasing praseodymium additions to ceria-yttria. In contrast, Tb additions to yttria-doped ceria do not result in any significant microstructural change. Although an increase in grain conductivity with small amounts of Pr was observed at 300ºC, both co-dopants exert a deleterious effect on the electrical conductivity of YDC at typical operation temperatures for solid oxide fuel cells.

Introduction

Solid electrolytes exhibiting high oxygen-ion conductivity are of special interest for applications in electrochemical devices such as oxygen sensors, oxygen separation membranes and solid oxide fuel cells, SOFCs (1,2). Solid solutions of ceria and other rare earths have been regarded as promising electrolytes for intermediate temperature (IT) SOFC operation because of their high ionic conductivity (3-6). The major restriction associated to these electrolytes is the increase of the electronic conductivity at high temperatures and low oxygen partial pressures due to the reduction of Ce^{4+} to Ce^{3+}. One approach to overcome this problem is the use of a co-dopant. In principle, the minority dopant should be able to enlarge the electrolytic domain and/or to increase the ionic conductivity of ceria-based solid solutions. A few rare earth cations have attracted specific attentions (5,7-11).

In previous studies, the solid electrolytes were prepared by different methods like the solid state reaction (8,11), coprecipitation (12), and the hydrothermal method (10), which can give rise to different microstructures. In this work, solid solutions were synthesized by coprecipitation to verify the effect of praseodymium and terbium co-additions on microstructural and electrical properties of of yttria-doped ceria solid electrolytes.

Experimental

Cerium nitrate hexahydrate (99.99%, Aldrich), yttrium oxide (99.99%, Sigma Chem. Co), praseodymium oxide (99.9%, Aldrich), and terbium nitrate (99.9%, Alfa Aesar)

were used as starting materials. The concentration of stock solutions of the corresponding metal nitrates was determined by gravimetric analysis. The hydroxide coprecipitation method was used to synthesize $Ce_{0.85}Y_{0.15-x}Pr_xO_{2-\delta}$ and $Ce_{0.85}Y_{0.15-x}Tb_xO_{2-\delta}$ with x = 0.02 and 0.06 solid solutions and $Ce_{0.85}Y_{0.15}O_{2-\gamma}$ solid electrolytes. For comparison purposes, $Ce_{0.85}Y_{0.13}Pr_{0.02}O_{2-\delta}$ was prepared by mixing Pr_6O_{11} to the coprecipitate of ceria-yttria. Further details on the hydroxide coprecipitation method may be found elsewhere (13,14). Cylindrical pellets were prepared with calcined powders by uniaxial pressing and sintering at 1450ºC for 4 h.

The apparent density of sintered pellets was determined by the immersion method. Raman spectroscopy (Renishaw Raman Microscope System 3000) was used for structural characterization. The morphology of polished and thermally etched surfaces was observed by scanning electron microscopy (Philips, XL30). Semi-quantitative elemental analysis on selected micro-regions of sintered pellets was performed by energy dispersive spectroscopy (EDS). The mean grain size was estimated by the intercept method. Electrical conductivity measurements were carried out by impedance spectroscopy using a low-frequency impedance analyzer (HP 4192A) in the 5 Hz to 13 MHz frequency range. Silver was used as the electrode material.

Results and Discussion

All sintered pellets had relative densities higher than 95% independent of co-dopant type and content. Therefore, no corrections for porosity were carried out.

Influence of the Method of Synthesis

Raman spectra were recorded at several micro-regions of sintered pellets for structural characterization. Fig. 1 shows typical Raman spectra. Pellets prepared from coprecipitated powders (Fig. 1a) exhibit a high intensity Raman band centered at ~ 467 cm^{-1}, which is characteristic of the cubic structure. In addition, two superimposed low intensity bands in the 500 to 650 cm^{-1} spectral range are assigned to the oxygen vacancies, created as charge compensating defects. Fig. 1 (b) and (c) are Raman spectra of sintered pellets prepared by mixing Pr_6O_{11} to the ceria-yttria mixed hydroxide powder. Some micro-regions (designated A) have a spectrum similar to that of Fig. 1a. One of them is shown in Fig. 1 b. However, other micro-regions (designated B) exhibit a Raman spectrum like that in Fig. 1c. In this case, the Raman band with maximum amplitude at ~ 570 cm^{-1} may be identified as that characteristic of the solid solution formed between cerium oxide and praseodymium oxide (15). This result evidences that praseodymium oxide segregated during the processing of powders and reacted with cerium oxide during sintering to form a praseodymium rich solid solutions.

Fig. 2 shows the EDS spectrum of one micro-region corresponding to the segregated phase. It is worth noting the relative low content of yttrium in the segregated phase. The average contents of Ce, Y and Pr determined in several micro-regions are listed in Table 1. These results showed that the dispersion of the co-dopant was not uniform for powders prepared by the conventional method, resulting in lack of chemical homogeneity in the sintered pellets. This effect, in turn, may be responsible for microstructure dependence of

the electrical conductivity. Fig. 3 shows the Arrhenius plots of the electrical conductivity of pellets prepared by different methods and for $Ce_{0.85}Y_{0.15}O_{2-\gamma}$ designated as standard.

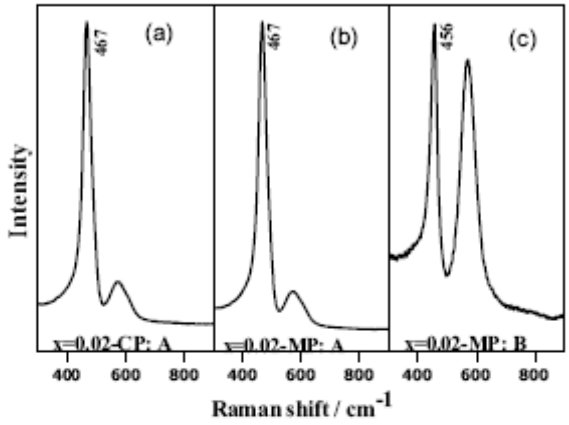

Figure 1. Raman spectra of sintered pellets prepared from coprecipitated (CP) (a), and mixing of oxide (MP) powders (b and c).

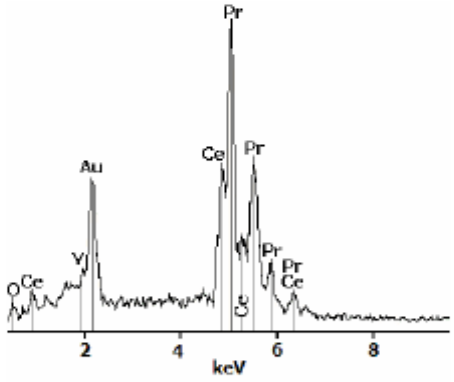

Figure 2. EDS spectrum of the segregated phase.

Table I. Elemental analysis determined by EDS on sintered pellets prepared by coprecipitation (CP) and mixing of powders (MP).

Element	CP pellet (at.%)	MP pellet (at.%)	MP pellet * (at.%)
Ce	84.3	84.6	~45
Y	13.8	14.1	<1
Pr	1.9	1.3	~54

* segregated phase.

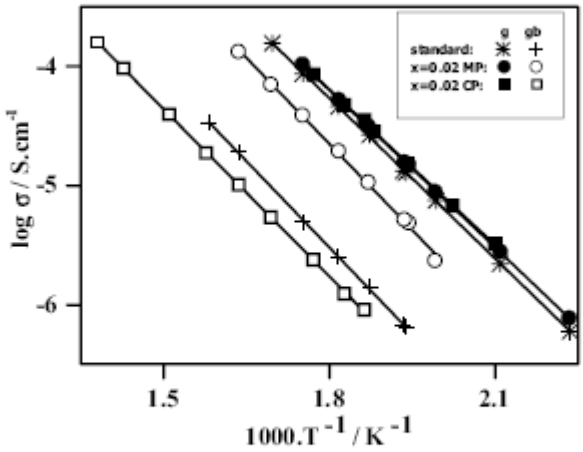

Figure 3 An Arrhenius plot of grain (g) and grain boundaries (gb) conductivities (σ) of $Ce_{0.85}Y_{0.13}Pr_{0.02}O_{2-\delta}$ prepared by different methods and $Ce_{0.85}Y_{0.15}O_{2-\gamma}$ (standard) pellet.

As shown in Fig. 3, the grain conductivity is almost unaffected by the method of synthesis. Moreover, the grain conductivity of pellets containing Pr as co-dopant is slightly higher than that of yttria-doped ceria. The grain boundary conductivity, in contrast, greatly differs in these samples. The higher grain boundary conductivity of the pellet prepared by mixing of powders is probably related to an increased electronic conductivity due to the ceria-praseodymia segregated phase.

Influence of Co-Dopant Type and Content

To study the effect of co-dopant type and content, all samples were prepared by the coprecipitation method to ensure the chemical homogeneity of sintered materials. Table II shows the calculated mean grain size (G) for the studied compositions. Increasing Pr additions produces a decrease in the mean grain size of sintered pellets, whereas for Tb additions the grain size is almost unchanged. Values of the apparent activation energies for grain and grain boundary conductivities are also listed in Table II. It can be seen that a decrease in activation energy with increasing co-dopant content. However, at the temperature range of measurements where the ionic component is predominant, the small decrease of the activation energy for the grain component may be related to a beneficial effect of Pr in the microstructural homogeneity.

Table II. Values of mean grain size (G) and apparent activation energy (E) for grains (g) and grain boundaries (gb).

Parameter	standard	0.02 Pr	0.06 Pr	0.02 Tb	0.06 Tb
G (μm)	1.6	1.4	1.1	1.4	1.5
E_g (eV)	0.87	0.84	0.74	0.87	0.79
E_{gb} (eV)	0.94	0.91	0.85	0.92	0.84

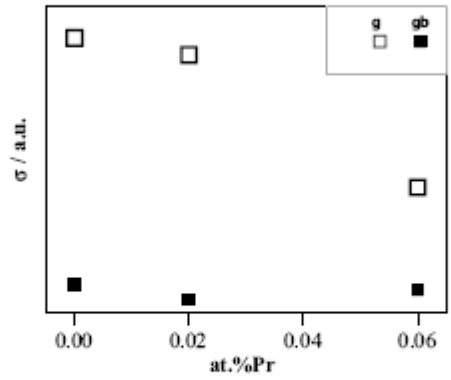

Figure 4. Estimated values of grain and grain boundary conductivity at 650ºC for Pr co-additions.

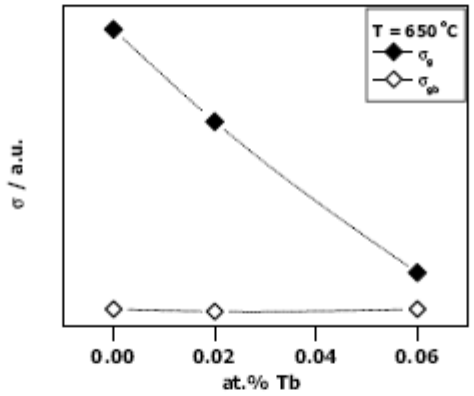

Figure 5. Estimated values of grain and grain boundary conductivity at 650ºC for Tb co-additions.

Fig. 4 shows estimated values of grain and grain boundary conductivity at 650°C, a possible operation temperature for IT SOFCs. It can be seen that the grain conductivity decreases with increasing Pr content, in contrast to what was obtained at 300°C. Fig. 5 shows that Tb co-additions remarkably decrease the grain conductivity. Therefore, both Pr and Tb co-dopants have a deleterious effect at intermediate temperatures.

Conclusions

Chemically homogeneous solid electrolytes of yttria-doped ceria containing small additions of Pr and Tb were obtained by the hydroxide coprecipitation method. These co-dopants have a deleterious effect at intermediate temperatures. Small Pr additions may be valuable for SOFC operation at low temperatures.

Acknowledgments

The authors acknowledge FAPESP, CNEN and CNPq for financial support. S. K. Tadokoro acknowledges FAPESP for the scholarship.

References

1. J. B. Goodenough, A. Manthiram, M. Paranthaman and T. S. Zhen, *Mater. Sci. Eng.*, **B12**, 357 (1992).
2. N. Q. Minh, *J. Am. Ceram. Soc.*, **76**, 563 (1993).
3. H. Inaba and H. Tagawa, *Solid State Ionics*, **83**, 1 (1996).
4. R. Doshi, V. L. Richards, J. D. Carter, X. Wang and M. Krumpelt, *J. Electrochem. Soc.*, **146**, 1273 (1999).
5. B. C. H. Steel, *Solid State Ionics*, **129**, 95 (2000).
6. V. V. Kharton, F. M. Figueiredo, L. Navarro, E. N. Naumovich, A. V. Kovalevsky, A. A. Yaremchenko, A. P. Viskup, A. Carneiro, F. M. B. Marques and J. R. Frade, *J. Mater. Sci.*, **36**, 1105 (2001).
7. D. L. Maricle, T. E. Swarr and S. Karavolis, *Solid State Ionics*, **52**, 173 (1992).
8. N. Maffei and A. K. Kuriakose, *Solid State Ionics*, **107**, 67 (1998).
9. N. Kim, B.-H. Kim and D. Lee, *J. Power Sources*, **90**, 139 (2000).
10. W. Huang, P. Shuk and M. Greenblatt, *J. Electrochem. Soc.*, **147**, 439 (2000).
11. V. V. Kharton, A. P. Viskup, F. M. Figueiredo, E. N. Naumovich, A. L. Shaulo and F. M. B. Marques, *Mater. Lett.*, **53**, 160 (2002).
12. D. L. Maricle, T. E. Swarr and H. L. Tuller, US Patent, 5,001,021 (1991).
13. S. K. Tadokoro and E. N. S. Muccillo, *J. Alloys Comp.*, **374**, 190 (2004).
14. S. K. Tadokoro and E. N. S. Muccillo, *J. Eur. Ceram. Soc.*, accepted.
15. J. R. McBride, K. C. Hass, B. D. Poindexter and W. H. Weber, *J. Appl. Phys.*, **76**, 2435 (1994).